BIOTECHINTELECT, 2026, 3 (1) e10 (1-16)

https://jbiotechintel.com/index.php/biotechintel

Research Article

eISSN: 3115-7920

OPEN ACCESS

Curcumin-Loaded Mesoporous Silica Nanoparticle-Embedded Injectable Thermoresponsive Chitosan Hydrogel for Sustained Drug Delivery

Mitra Asadian[1], Ladan Rashidi[2]*, Fariba Ganji[3]*

[1] Department of Biomaterials, Faculty of Interdisciplinary Sciences and Technologies, Tarbiat Modares University, 14115-336, Tehran, Iran
[2] Department of Food and Agricultural Products, Food Technology and Agricultural Products Research Center, Standard Research Institute (SRI), Karaj, I.R. IRAN, PO Box 31745-139, Karaj, Iran
[3]Biomedical Engineering Group, Faculty of Chemical Engineering, Tarbiat Modares University, PO Box 14115-143, Tehran, Iran

Article history:
Received 08 March 2026
Revised 18 April 2026
Accepted 23 April 2026
Published online 25 April 2026

Keywords: Chitosan Injectable Hydrogel, Curcumin, Mesoporous Silica Nanoparticles, Cell Uptake.

How to cite this article: Asadian, M., Rashidi, L., Ganji, F. Curcumin-Loaded Mesoporous silica nanoparticle-embedded injectable thermoresponsive chitosan hydrogel for sustained drug delivery, *Biotech-Intellect,* 2026; 3(1): e10, 1-16.

https://doi.org/10.66224/BiotechIntellect.3.1.51

*corresponding author's email:
Ladan Rashidi
l.rashidi@standard.ac.ir
Tel.: 98 21 82884383, Fax: 98 21 82884931,
Fariba Ganji
fganji@modares.ac.ir

ABSTRACT

Background and Aim: Curcumin as natural bioactive compound with therapeutic potential; however, has limited clinical application due to poor aqueous solubility, low bioavailability, and rapid metabolism. This study aimed to develop an injectable thermoresponsive chitosan/β-glycerophosphate hydrogel incorporating curcumin-loaded mesoporous silica nanoparticles to achieve sustained local delivery of curcumin.

Methods: MSNs were synthesized, loaded with curcumin, and dispersed into a chitosan/β-glycerophosphate solution to prepare an injectable in situ gelling hydrogel. The prepared formulations were characterized by Fourier transform infrared, X-Ray Diffraction, nitrogen adsorption–desorption analysis, and field-emission scanning electron microscopy. Curcumin loading capacity and entrapment efficiency were determined, while in vitro drug release was evaluated in simulated body fluid (pH 7.4). Biocompatibility was assessed on healthy primary human mammary fibroblasts, and cellular uptake was examined by transmission electron microscopy using Michigan Cancer Foundation-7 cells.

Results and Discussion: The loading capacity and entrapment efficiency of MSNs-curcumin were 20 wt% and 78 wt%, respectively. Characterization confirmed successful incorporation of curcumin into the MSNs and their uniform distribution within the hydrogel network. The chitosan/β-glycerophosphate/MSNs-curcumin hydrogel exhibited a prolonged curcumin release profile with minimal initial burst release under physiological conditions. MTT assay demonstrated that both MSNs-curcumin and chitosan/β-glycerophosphate/MSNs-curcumin maintained over 90% viability of HPHMF cells after 24 and 48 h, indicating good biocompatibility. Transmission electron microscopy analysis confirmed successful cellular internalization of MSNs-curcumin by Michigan Cancer Foundation-7 cells. These findings suggest that the developed injectable hydrogel is a promising platform for sustained localized delivery of curcumin and other hydrophobic therapeutic agents.

What is "already known":

- MSNs as drug carriers due to their high loading capacity, large surface area, and tunable pore structure.
- Injectable thermoresponsive chitosan/β-glycerophosphate hydrogels as localized and sustained drug delivery owing to their excellent biocompatibility and in situ gel-forming capability.

What this article adds:	• An injectable thermoresponsive chitosan/β-glycerophosphate hydrogel incorporating curcumin-loaded MSNs as a dual sustained drug delivery platform. • Prolonged curcumin release with minimal initial burst release while maintaining excellent biocompatibility toward healthy fibroblasts. • Successful cellular internalization of the nanoparticles, supporting the potential of this hydrogel-based system for localized delivery of hydrophobic therapeutic agents.

1. INTRODUCTION

Nanoencapsulation technology has emerged as an effective strategy for improving the delivery of bioactive compounds. Encapsulation of therapeutic agents within nanostructures protects them from degradation during gastrointestinal digestion and cellular metabolism while enabling controlled drug release. In addition, nanoencapsulation can improve drug biodistribution, bioavailability, and targeted delivery to specific tissues [1].

Curcumin, a natural polyphenolic compound extracted from the rhizome of *Curcuma longa*, has attracted considerable attention because of its broad pharmacological activities. It has been reported to exhibit antibacterial, anticancer, anti-inflammatory, and antioxidant properties [2]. Despite these promising biological activities, the clinical application of curcumin is limited by its poor aqueous solubility, low absorption, rapid metabolism, short biological half-life, and consequently low bioavailability [3]. Various drug delivery strategies, including nanoparticles, liposomes, and polymeric micelles, have therefore been developed to overcome these limitations [4].

Among the available nanocarriers, mesoporous silica nanoparticles (MSNs) have attracted considerable attention owing to their unique structural characteristics and broad biomedical applications [5–7]. Their high surface area, large pore volume, tunable pore size, excellent thermal stability, and remarkable drug-loading capacity make them attractive carriers for a wide range of therapeutic agents. Moreover, MSNs generally exhibit favorable biocompatibility and are therefore considered promising materials for controlled drug delivery [8]. Nevertheless, their biosafety is influenced by several physicochemical parameters, including particle size, morphology, surface chemistry, concentration, and exposure time, while increased cytotoxicity has mainly been reported for unmodified silica surfaces or at relatively high concentrations [9]. More recently, Ribeiro et al. developed curcumin-loaded MSNs dispersed in a thermo-responsive hydrogel for intranasal treatment of Alzheimer's disease [10]. Their formulation exhibited high curcumin encapsulation efficiency together with favorable rheological and mucoadhesive properties, resulting in enhanced nasal permeation and improved therapeutic efficacy in an Alzheimer's disease model. However, this platform was specifically designed for intranasal administration and did not address the requirements of injectable in situ localized drug delivery [10].

Chitosan is a naturally derived amino-polysaccharide that has been extensively used in drug delivery systems because of its biodegradability, biocompatibility, low toxicity, and high hydrophilicity. Moreover, its abundant amino and hydroxyl functional groups facilitate chemical modification and interaction with a variety of nanomaterials [11]. Ahmadi Nasab et al. successfully developed chitosan-coated MSNs for curcumin delivery, demonstrating improved stability, solubility, bioavailability, and anticancer activity of curcumin [12]. Their study also investigated pH-dependent drug release in phosphate-buffered saline (PBS) at pH 5.5 and 7.4 and evaluated the cytotoxicity of the developed nanocarrier against U87MG glioblastoma cells. The results suggested that chitosan-coated MSNs could serve as a pH-responsive nanocarrier for controlled curcumin release in the acidic tumor microenvironment [12]. However, this delivery system did not provide injectable localized administration or in situ gel formation for prolonged drug retention at the target site.

Injectable in situ-forming hydrogels have recently attracted increasing interest as localized drug delivery

platforms. Chitosan/β-glycerophosphate (CS/βGP) thermosensitive hydrogels remain in the sol state at room temperature and undergo rapid gelation under physiological conditions. This unique behavior enables minimally invasive administration while providing sustained local drug release [13]. β-Glycerophosphate (βGP) is an organic phosphate salt that acts as a pH-adjusting agent for chitosan solutions. When mixed with chitosan, βGP neutralizes the acidic solution to near physiological pH without inducing immediate gelation. Gel formation occurs only after exposure to body temperature, making this system particularly attractive for injectable drug delivery applications [14].

Although MSNs and thermosensitive chitosan hydrogels have shown considerable potential as independent drug delivery platforms, the development of a hybrid injectable system combining curcumin-loaded MSNs with a CS/βGP thermoresponsive hydrogel remains insufficiently explored. Previous studies have primarily focused either on improving curcumin solubility and bioavailability using nanoparticle-based systems or on achieving sustained drug release using injectable hydrogels. However, the synergistic contribution of nanoparticle encapsulation and in situ hydrogel formation toward minimizing initial burst release, enhancing local drug retention, and maintaining biocompatibility has not been comprehensively investigated. Therefore, the present study aimed to develop an injectable thermoresponsive CS/βGP hydrogel incorporating curcumin-loaded MSNs (MSNs-CU) as a hybrid sustained drug delivery platform. The release profiles of MSNs-CU, curcumin-loaded CS/βGP hydrogel (CS/βGP/CU), and MSNs-CU incorporated within the CS/βGP hydrogel (CS/βGP/MSNs-CU) were comparatively evaluated in simulated body fluid (SBF, pH 7.4). Furthermore, the biocompatibility of MSNs, CS/βGP hydrogel and CS/βGP/MSNs was assessed using primary human mammary fibroblasts (HPHMF) by the MTT assay. Finally, transmission electron microscopy (TEM) was used to investigate the cellular uptake of MSNs-CU by Michigan Cancer Foundation-7 (MCF-7) human breast cancer cells.

2. MATERIAL AND METHODS

2.1. Materials

Tetraethyl orthosilicate, *N*-cetyltrimethylammonium bromide, hydrochloric acid (HCl, 37%), acetic acid, mesitylene (98%), sodium hydroxide (NaOH), acetonitrile, and ethanol were purchased from Merck (Germany). Curcumin, trypsin solution, glutaraldehyde (8% aqueous solution), β-glycerophosphate (βGP), chitosan (low molecular weight, degree of deacetylation >90%), 3-(4,5-dimethylthiazol-2-yl)-2,5-diphenyltetrazolium bromide (MTT), and phosphate-buffered saline (PBS) were obtained from Sigma-Aldrich (USA). Dulbecco's Modified Eagle Medium (DMEM), penicillin–streptomycin antibiotic solution, and fetal bovine serum (FBS) were purchased from Gibco BRL (Gaithersburg, USA). All solutions were prepared using deionized water. Simulated body fluid (SBF, pH 7.4) was prepared according to the method previously described [9].

2.2 MSNs synthesis

MSNs were synthesized according to the method previously reported by Rashidi et al. [9]. Briefly, 3.5 mL of 2.0 M NaOH solution and 1.0 g of *N*-cetyltrimethylammonium bromide were dissolved in 480 mL of deionized water and heated to 80°C under continuous stirring. After the reaction temperature reached 80°C, mesitylene was added, and the mixture was stirred for 5 h. Subsequently, 5 mL of tetraethyl orthosilicate was added dropwise at a rate of 1 mL min^{-1}. The reaction mixture was further stirred for an additional 2 h. The resulting MSN suspension was filtered through a 0.45 µm polypropylene membrane filter, washed thoroughly with a water/ethanol mixture, and dried under vacuum. Finally, the dried product was calcined at 540°C for 4 h using a heating rate of 1°C min^{-1} to remove the surfactant template [7].

2.3. Loading capacity and entrapment efficiency

To determine the optimal curcumin loading conditions into MSNs, different concentrations of curcumin in ethanol (0, 1, 2, 3, and 4 mg mL^{-1}) were prepared. Then, 10 mg of MSNs was added to 1 mL of each curcumin solution, resulting in initial curcumin/MSNs (CU/MSNs) weight ratios of 0, 0.1, 0.2, 0.3, and 0.4, respectively. The suspensions were stirred at 200 rpm for 24 and 48 h. After incubation,

3

the samples were centrifuged at 9,400 × g for 5 min, and the clear supernatants were collected. To remove the remaining unencapsulated curcumin from the nanoparticle surface, 1 mL of ethanol was added to the precipitates, followed by a second centrifugation step. This washing procedure was repeated twice. The collected supernatants were combined for quantitative determination of the amount of curcumin incorporated into the MSN pores. The curcumin-loaded nanoparticles were subsequently dried under vacuum at 25°C. The amount of curcumin in the collected supernatants was determined using high-performance liquid chromatography (HPLC) equipped with a UV detector at a wavelength of 425 nm [4]. The curcumin loading capacity (LC%) and entrapment efficiency (EE%) were calculated using Eq.1 & 2 [15]:

$$\mathrm{DL}(\%) = \frac{\text{weight of loaded curcumin}}{\text{weight of curcumin loaded nanoparticles}} \times 100\% \quad \text{(Eq.1)}$$

$$\mathrm{EE}(\%) = \frac{\text{weight of loaded curcumin}}{\text{initial weight of curcumin}} \times 100\% \quad \text{(Eq.2)}$$

2.4. HPLC conditions for curcumin quantification

The curcumin was determined using HPLC system (Young Lin 9100, Young Lin Instrument Co., Korea) equipped with a quaternary pump and UV detector. Chromatographic separation was performed using a reversed-phase Athena C18-WP column (4.6 mm × 250 mm, 100 Å, 5 µm).

The mobile phase consisted of solvent A, containing distilled water with 0.1% (v/v) citric acid adjusted to pH 3, and solvent B, acetonitrile. The analysis was performed using an A/B ratio of 50:50 (v/v) for 60 min under isocratic conditions. The mobile phases were degassed before analysis, and the flow rate was maintained at 1.0 mL min^{-1}. The UV detector was set at 425 nm for the quantitative determination of curcumin concentration [16].

2.5. Preparation of injectable thermosensitive CS/βGP hydrogel

The thermosensitive injectable hydrogel system was prepared using chitosan (2% w/v) and β/GP (8% w/v). Briefly, 100 mg of chitosan powder was dissolved in 4.5 mL of 0.1 M hydrochloric acid solution. The chitosan solution was maintained in an ice-water bath at 4°C to prevent premature gelation during preparation. For preparation of curcumin-loaded CS/βGP hydrogel (CS/βGP/CU), 22 mg of curcumin (corresponding approximately to the amount of curcumin present in 100 mg of MSNs-CU) was gradually added to the cold chitosan solution under vigorous stirring until a homogeneous dispersion was obtained. Subsequently, 800 mg of βGP was slowly added to the chitosan/curcumin mixture while continuously stirring at 4°C. The resulting solution was incubated at 37°C to evaluate hydrogel formation. For preparation of CS/βGP hydrogel containing curcumin-loaded MSNs (CS/βGP/MSNs-CU), 100 mg of MSNs-CU containing the equivalent amount of curcumin was dispersed into the CS/βGP solution under continuous stirring. A blank CS/βGP hydrogel without curcumin or nanoparticles was prepared using the same procedure and used as the control formulation [14].

2.6. Sample Characterization

The specific surface area, pore size distribution, and pore volume of the MSNs were determined using a Micromeritics ASAP 2010 surface area analyzer. The specific surface area was calculated according to the Brunauer–Emmett–Teller (BET) method over the relative pressure (P/P_0) range of 0.20–0.40. The morphology of the synthesized MSNs was examined using field-emission scanning electron microscopy (FE-SEM; Philips XL-30). Prior to imaging, the samples were sputter-coated with a thin carbon layer to improve conductivity. X-Ray Diffraction (XRD) analysis was performed to confirm the hexagonal structure of the synthesized nanoparticles. MSNs exhibit characteristic reflections at low diffraction angles. The low-angle XRD pattern of the mesoporous silica nanoparticles was recorded over a 2θ range of 0° to 10°. For the analysis, the sample was placed on a glass substrate, and X-rays with a wavelength of 1.5 Å were used for diffraction measurements. The 2θ angle was varied from 1° to 10° with a step size of 0.02°. Here, 2θ represents the angle between the incident and diffracted X-ray beams, whereas θ is the angle between the incident X-ray beam and the plane of the sample surface. For morphological evaluation of the hydrogel formulations, 1 mL of CS/βGP/MSNs-CU or blank CS/βGP/MSNs hydrogel was transferred into separate vials and frozen at −80°C. The frozen samples were subsequently freeze-dried at −50°C under a vacuum of 0.1 mbar for 3 h. The lyophilized samples were then observed by FE-SEM. Fourier transform infrared (FTIR) spectra of all samples were

recorded using an FTIR spectrometer (PerkinElmer, USA) employing the KBr pellet method. The cellular uptake of MSNs-CU and CS/βGP/MSNs-CU by MCF-7 human breast cancer cells was evaluated using TEM (Philips CM120) [7].

2.7. In vitro curcumin release

For the in vitro release study, 10 mg of MSNs-CU was weighed and dispersed in 1 mL of simulated body fluid (SBF, pH 7.4). A blank sample consisting of 10 mg of unloaded MSNs in 1 mL of SBF was prepared as the control. The vials were incubated in a shaking water bath at 37°C with continuous agitation at 100–120 rpm. At predetermined time intervals, the samples were centrifuged at 9,400 × g for 5 min. The supernatants were carefully collected and analyzed by HPLC to determine the amount of released curcumin. An equal volume of fresh SBF was added after each sampling to maintain a constant release volume throughout the experiment. To evaluate curcumin release from the hydrogel formulations, 5 mL of each hydrogel precursor suspension (CS/βGP/MSNs-CU and CS/βGP/CU) was transferred into separate flasks and incubated at 37°C until complete gelation occurred. Subsequently, 10 mL of SBF (pH 7.4) was gently added onto the surface of each hydrogel. The flasks were maintained at 37°C on a shaker operating at 120 rpm. At predetermined sampling intervals, aliquots of the release medium were withdrawn and analyzed by HPLC for curcumin quantification. After each sampling, an equal volume of fresh SBF was added to maintain a constant release volume throughout the experiment. The cumulative amount of released curcumin was calculated by considering both the amount of drug present in the release medium at each sampling point and the amount removed in the previous samples. The cumulative release profiles were then plotted as a function of time [17].

2.8. Biocompatibility of the prepared samples

The in vitro biocompatibility of the prepared formulations was evaluated using the MTT assay on healthy primary human mammary fibroblast (HPHMF) cells. HPHMF cells were obtained from the National Institute for Genetic Engineering and Biotechnology (Tehran, Iran). The cells were cultured in Dulbecco's Modified Eagle Medium (DMEM; 4.5 g/L glucose) supplemented with 10% FBS, penicillin (100 IU/mL), streptomycin (100 µg/mL), and 1% L-glutamine (200 mM). The cells were maintained in a humidified incubator at 37°C with 5% CO_2 and 95% relative humidity. The culture medium was refreshed every 3–4 days. The biocompatibility of MSNs, CS/βGP and CS/βGP/MSNs was investigated using the MTT assay. Briefly, HPHMF cells were seeded into 96-well plates and incubated until appropriate cell attachment was achieved. Subsequently, the culture medium was replaced with fresh medium containing different concentrations (10–500 µg/mL) of the prepared samples. After 24 and 48 h of incubation, the treatment media were removed and replaced with fresh medium containing MTT solution (5 mg/mL). The cells were incubated for an additional 4 h at 37°C to allow the formation of formazan crystals. The supernatant was then removed, and 100 µL of DMSO was added to each well to dissolve the crystals. The absorbance of each well was measured at 570 nm using a Multiskan Spectrum microplate reader (Thermo Fisher Scientific). The percentage of viable cells was calculated relative to untreated control cells using the Eq. 3:

$$\text{Cell viability [\%]} = 100 \times \frac{\text{Abs}_{570}\ (\text{Treated Cells})}{\text{Abs}_{570}\ (\text{Control Cells})} \quad \text{(Eq.3)}$$

where Abs_{570} is absorbance at 570 nm [18].

2.9. TEM evaluation of MSNs-CU internalization in MCF-7 Cells

MCF-7 human breast cancer cells were obtained from the National Institute for Genetic Engineering and Biotechnology (Tehran, Iran). The cells were cultured as a monolayer in T-75 flasks containing Dulbecco's Modified Eagle Medium (DMEM) supplemented with 10% (v/v) fetal bovine serum (FBS). Cell cultures were maintained at 37°C in a humidified atmosphere containing 5% CO_2 and 95% relative humidity. The cells were detached and adjusted to the desired concentration using a hemocytometer. Subsequently, MCF-7 cells were seeded into T-25 flasks at a density of 6×10^5 cells per flask and incubated overnight. The cells were then treated with CS/βGP/MSNs-CU suspension (100 µg/mL) and incubated for 24 h. After treatment, the culture medium was removed, and the cells were washed three times with PBS. The cells were subsequently collected by centrifugation at 1500 rpm for 5 min. The obtained cell pellets were fixed using a mixture of 2.5% (v/v) glutaraldehyde, 4% (v/v) paraformaldehyde, and 0.1 M PBS for 3 h. After fixation, the cell pellets were washed with 0.1 M PBS, embedded in 2% agarose gel, and post-fixed with 4%

osmium tetroxide solution for 1 h. The samples were then washed with distilled water and stained with 0.5% aqueous uranyl acetate for 1 h. Dehydration was performed using a graded ethanol series (10, 30, 60, 70, 90, and 100%). Finally, ultrathin sections (50–70 nm) were prepared using an ultramicrotome and subsequently stained with 5% aqueous uranyl acetate and 2% aqueous lead citrate before TEM observation [9].

2.10. Statistical Analysis

All experimental data were obtained from at least three independent measurements and are presented as mean ± standard deviation (SD). Statistical analysis was performed using one-way analysis of variance (ANOVA) followed by Tukey's post hoc test to determine significant differences among groups. A value of $p < 0.05$ was considered statistically significant.

3. RESULTS AND DISCUSSION

3.1. Characterization of MSNs nanoparticles

The FTIR spectra of MSNs and MSNs-CU are presented in Fig. 1a and 1b, respectively. The characteristic absorption bands of MSNs observed at approximately 801 and 1084 cm^{-1} correspond to the symmetric and asymmetric stretching vibrations of the Si–O–Si framework, confirming the formation of the silica network. The broad absorption band around 1630 cm^{-1} is mainly attributed to the bending vibration of adsorbed water molecules associated with surface silanol groups.

Following curcumin loading, noticeable changes in the FTIR spectrum were observed. The increased intensity of the absorption band around 1084 cm^{-1}, together with the appearance and enhancement of characteristic curcumin-related bands, suggests successful incorporation of drug into the mesoporous structure. The absorption band near 1629 cm^{-1} can be assigned to the conjugated carbonyl (C=O) and aromatic C=C stretching vibrations of curcumin, while the band at approximately 1570 cm^{-1} corresponds to the aromatic C=C stretching vibration of the benzene rings. Furthermore, the broad absorption region between 3000 and 3750 cm^{-1} is attributed to O–H stretching vibrations originating from the phenolic hydroxyl groups of curcumin and surface silanol groups, indicating possible hydrogen-bonding interactions between curcumin and the silica surface [19]. These spectral changes collectively support the successful loading of curcumin into the pores of the MSNs.

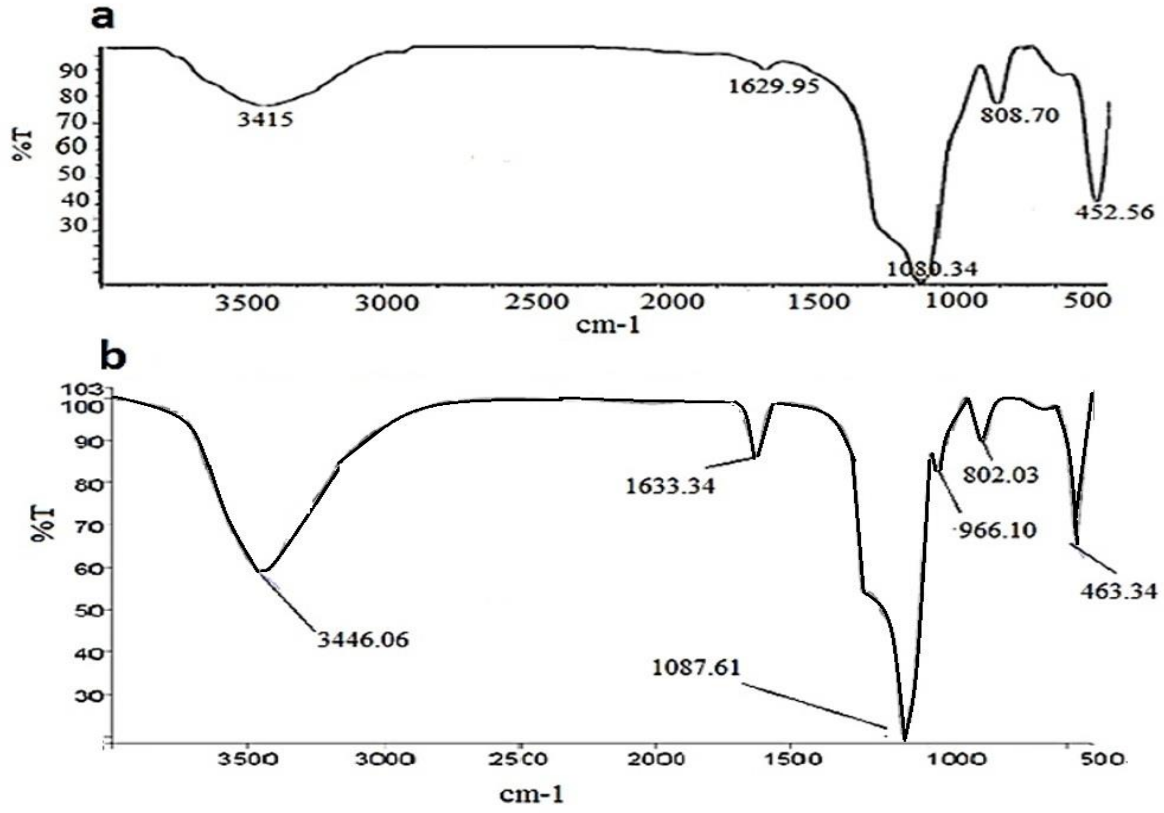

Fig.1. FTIR spectra of a) MSNs and b) MSNs-CU

The XRD patterns of MSNs and MSNs-CU are presented in Fig. 2. The characteristic diffraction peaks indexed to the (100), (110), (200), and (210) planes confirm the well-ordered hexagonal mesoporous structure of the synthesized MSNs. After curcumin loading, the diffraction pattern retained the characteristic (100) reflection, indicating that the ordered mesoporous framework remained intact. However, a noticeable decrease in the intensity of the diffraction peaks was observed following curcumin loading. In particular, the (200) and (210) reflections became indistinguishable, while the intensities of the (100) and (110) peaks were markedly reduced. These changes are consistent with the incorporation of curcumin into the mesoporous channels, which decreases the electron density contrast between the silica walls and the pore interiors. The attenuation and disappearance of the higher-order reflections further suggest partial filling of the mesopores and a reduction in long-range pore ordering after drug loading, while preserving the overall meso structure of the nanoparticles [20].

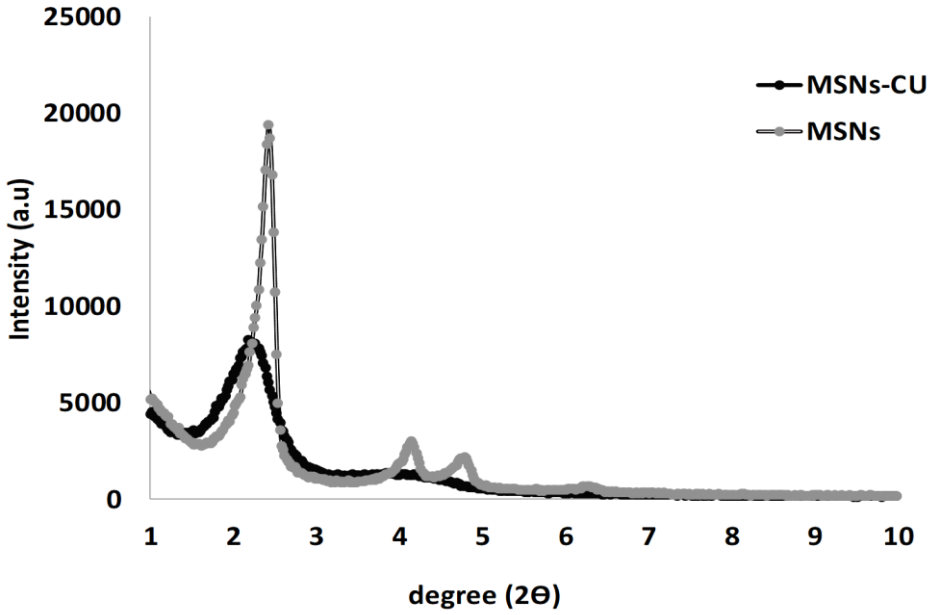

Fig.2. XRD patterns of MSNs and MSNs-CU

The textural properties of MSNs and MSNs-CU, obtained from nitrogen adsorption–desorption analysis, are summarized in Table 1. Following curcumin loading, the BET specific surface area decreased from 992.4 to 783.1 $m^2\ g^{-1}$, while the Barrett–Joyner–Halenda (BJH) adsorption pore volume decreased from 1.037 to 1.000 $cm^3\ g^{-1}$. A slight reduction in the average pore diameter, from 4.70 to 4.60 nm, was also observed. These changes are consistent with the incorporation of curcumin molecules into the mesoporous channels, resulting in partial occupation of the pore space and a consequent reduction in the accessible surface area and pore volume. The synthesized MSNs exhibited a high specific surface area (992.4 $m^2\ g^{-1}$) and an average pore diameter of 4.70 nm, confirming the successful preparation of a highly porous mesoporous silica structure suitable for drug loading.

Table 1. Barrett–Joyner–Halenda (BJH) and Brunauer–Emmett–Teller (BET) Parameters of MSNs and MSNs-CU

Sample	BET Surface area (m^2g^{-1})	BJH Adsorption volume of Pore (cm^3g^{-1})	Pore diameter (nm)	BJH Adsorption area of pore (m^2g^{-1})
MSNs	992.4	1.037	4.70	1251
MSNs-CU	783.11	1.00	4.60	922.7

3.2. Drug loading capacity and entrapment efficiency

LC and EE of curcumin were evaluated by incubating 10 mg of MSNs with different amounts of curcumin (0, 1, 2, 3, and 4 mg). The LC and EE values were calculated according to Equations (1) and (2). As shown in Fig. 3, the LC increased progressively with increasing initial curcumin concentration, indicating greater incorporation of the drug into the mesoporous structure. In contrast, the EE gradually decreased as the initial drug-to-carrier ratio increased, which can be attributed to the finite loading capacity of the MSNs. As the available adsorption sites within the mesopores approached saturation, an increasing proportion of the added curcumin remained unencapsulated. At the highest initial CU/MSNs weight ratio (0.4), the EE and LC reached 78% and 20 wt%, respectively. No statistically significant differences were observed between the LC and EE values obtained after 24 and 48 h of incubation ($p > 0.05$), indicating that adsorption equilibrium was achieved within the first 24 h.

These findings are comparable to those reported by Ribeiro et al. [10], who achieved an encapsulation efficiency of approximately 87.7% for curcumin-loaded MSNs incorporated into a thermoresponsive hydrogel. Although the EE obtained in the present study was slightly lower, both studies demonstrate the high loading capability of mesoporous silica nanoparticles toward hydrophobic compounds such as curcumin. The difference in EE may be attributed to variations in MSN physicochemical characteristics, including pore size, specific surface area, synthesis protocol, and drug-loading conditions. Moreover, the LC achieved in the present study (20 wt%) indicates that a substantial amount of curcumin was successfully incorporated into the mesoporous structure while maintaining a relatively high encapsulation efficiency, supporting the suitability of the prepared MSNs for subsequent incorporation into the injectable CS/βGP hydrogel.

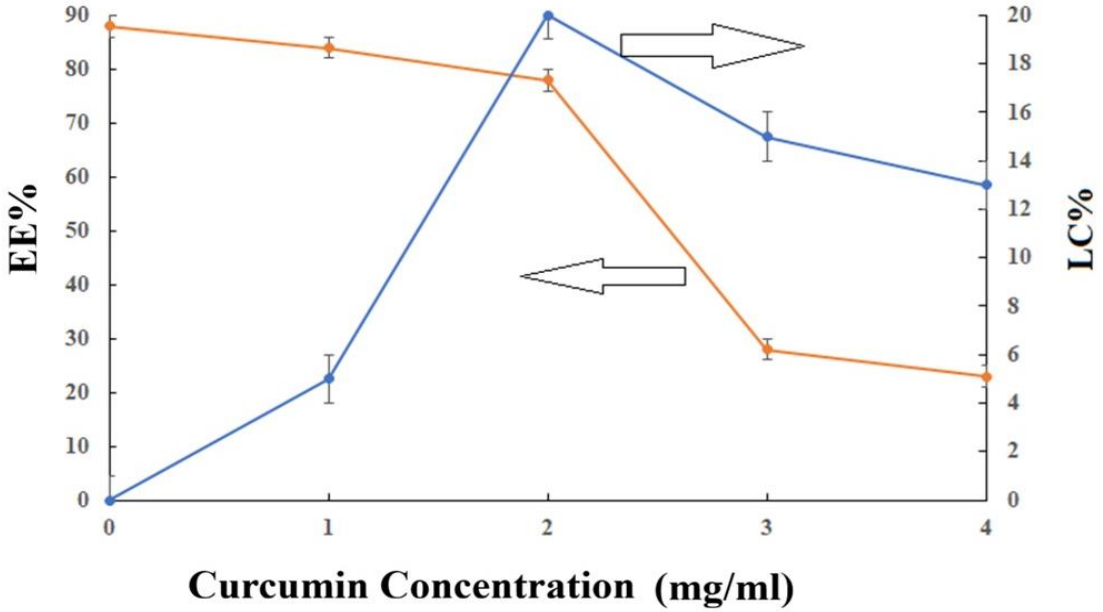

Fig. 3. Curcumin loading capacity (LC%) and entrapment efficiency (EE%)

3.3. Characterization of injectable hydrogels

The FTIR spectra of curcumin, CS/βGP hydrogel, CS/βGP/CU, and CS/βGP/MSNs-CU are presented in Fig. 4. The characteristic absorption bands observed at approximately 2859 and 2940 cm^{-1} correspond to the C–H stretching vibrations of the chitosan backbone. The spectra of CS/βGP, CS/βGP/CU, and CS/βGP/MSNs-CU also exhibited the characteristic amide I and amide II bands of chitosan at approximately 1671 and 1564 cm^{-1}, respectively.

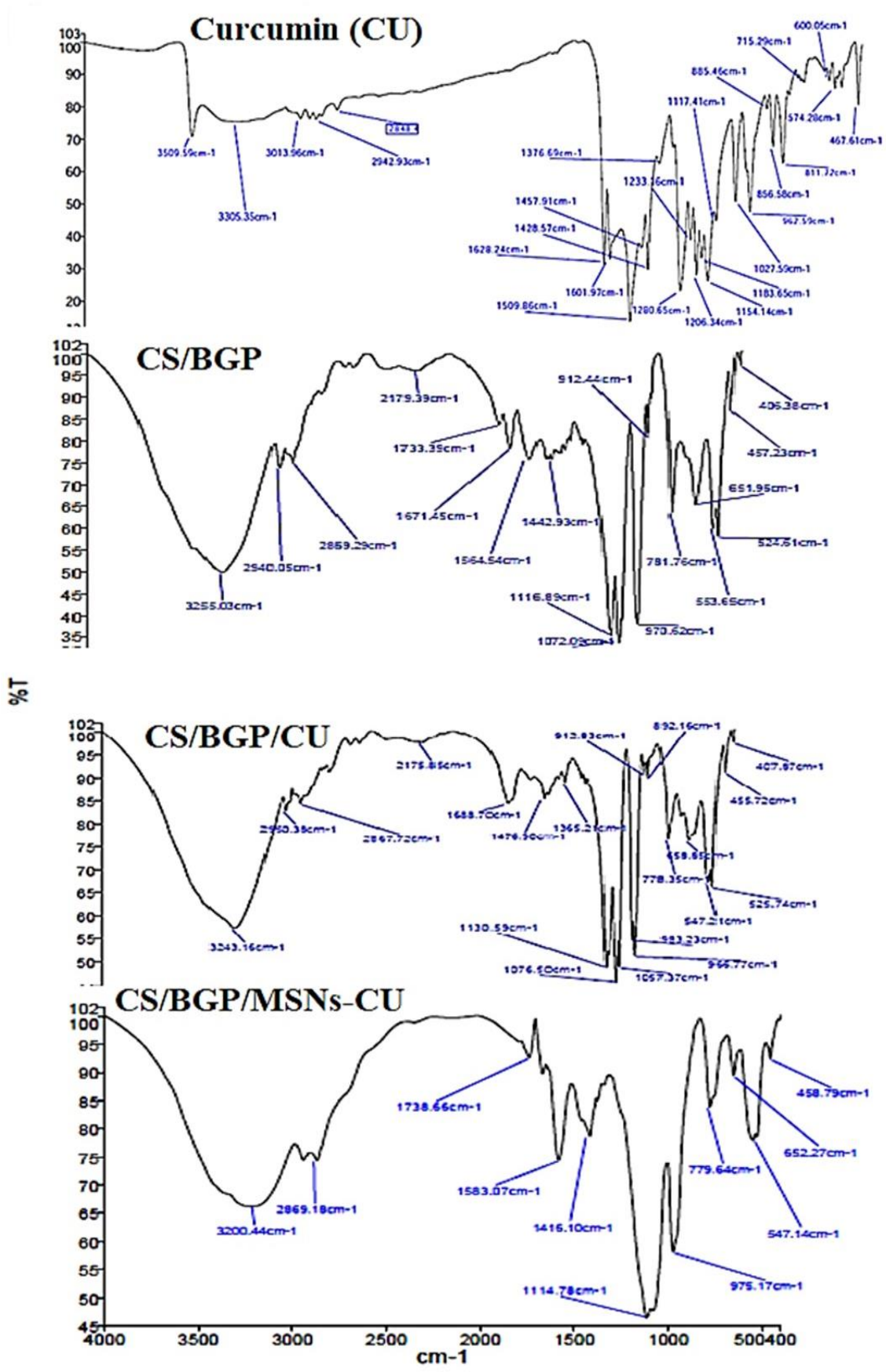

Fig.4. FTIR spectra of curcumin, CS/βGP, CS/βGP/CU, and CS/βGP/MSNs-CU

Following incorporation of CU-loaded MSNs into the hydrogel, the amide II band shifted from 1564 to 1583 cm^{-1} and exhibited increased intensity. This spectral shift suggests the presence of intermolecular interactions, most likely hydrogen bonding and electrostatic interactions, among chitosan, βGP, MSNs, and curcumin. The absorption bands observed at approximately 1442, 1365, and 1315 cm^{-1} are assigned to C–H bending and C–O stretching vibrations of the chitosan polymer backbone. In addition, the band detected at approximately 1416 cm^{-1} in the CS/βGP/MSNs-CU spectrum can be attributed to N–H bending vibrations, further indicating interactions between the hydrogel matrix and the incorporated nanoparticles. A broad absorption band between 3000 and 3750 cm^{-1}, corresponding to the stretching vibrations of hydroxyl (O–H) and amino (N–H) groups, showed a noticeable decrease in intensity after incorporation of MSNs-CU. This change is consistent with the formation of hydrogen-bonding interactions between the hydroxyl groups of curcumin, the surface silanol groups of MSNs, and the amino and hydroxyl groups of chitosan, confirming the successful integration of the drug-loaded nanoparticles within the hydrogel network [20].

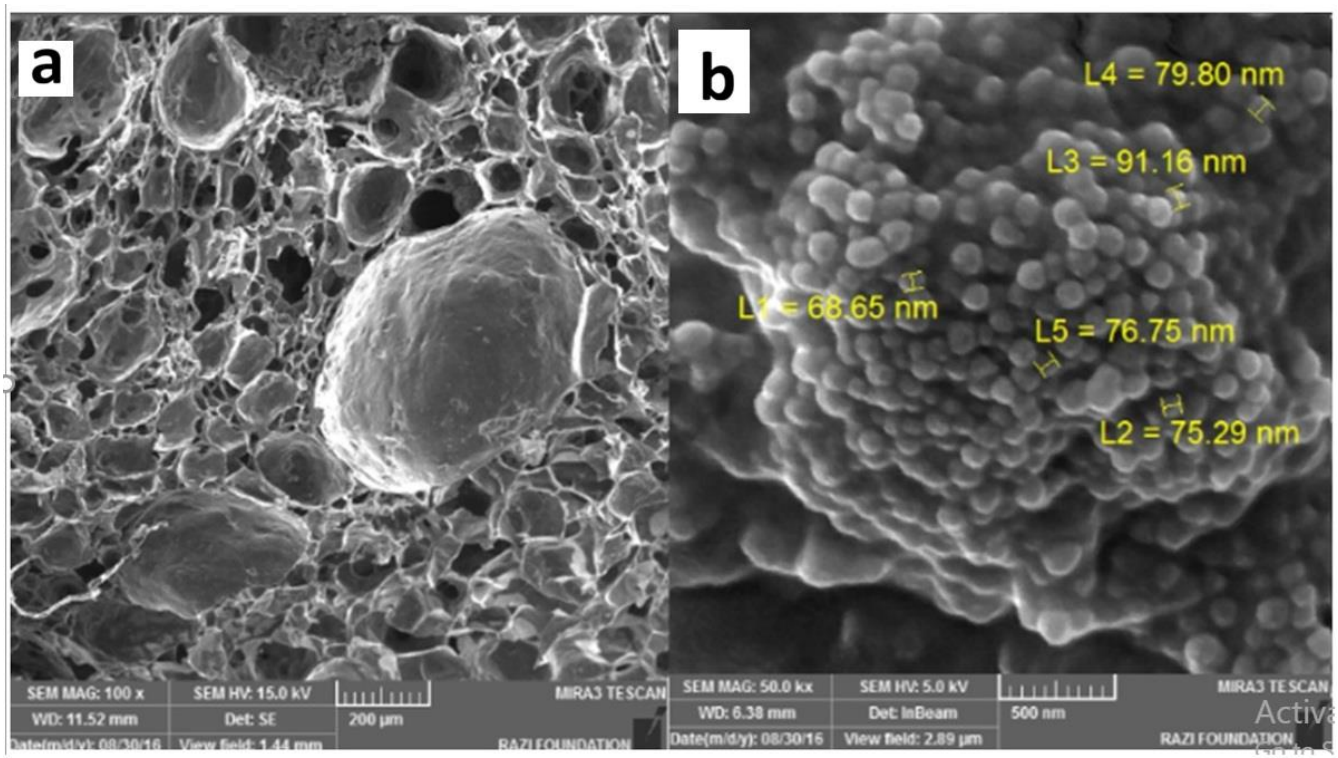

Fig. 5. SEM images of a) CS/βGP/MSNs-CU (100X) and b) CS/βGP/MSNs-CU (50000X)

Representative SEM images of the freeze-dried CS/βGP/MSNs-CU hydrogel is presented in Fig. 5. CS/βGP/MSNs-CU hydrogel exhibited a three-dimensional (3D) interconnected macroporous architecture with a honeycomb-like morphology. At higher magnification (Fig. 5b), the MSNs were observed to be uniformly dispersed throughout the hydrogel matrix, suggesting successful incorporation of the nanoparticles into the polymeric network. The nanoparticles retained their spherical morphology following encapsulation within the hydrogel.

The particle size of the incorporated MSNs ranged from approximately 61.7 to 91.2 nm, while the pore size of the freeze-dried hydrogels ranged from approximately 200 to 500 µm. The interconnected porous structure is expected to facilitate water penetration and mass transport within the hydrogel.

3.4. In Vitro curcumin release study

The cumulative release profile of curcumin from the CS/βGP/MSNs-CU hydrogel in simulated body fluid (SBF, pH 7.4) is presented in Fig. 6. During the first 20 h, approximately 5% of the encapsulated curcumin was

released, indicating the absence of a pronounced initial burst release. Thereafter, the release proceeded gradually, reaching approximately 36% after 120 h. Even after 220 h, more than 50% of the encapsulated curcumin remained within the hydrogel, demonstrating the ability of the developed system to provide prolonged and sustained drug release.

The sustained release profile observed in the present study is consistent with previous reports on curcumin-loaded mesoporous silica nanoparticles. For example, Ahmadi Nasab et al. [12] reported that, at pH 7.4, cumulative curcumin release reached approx.-imately 35% from uncoated MSNs and only 17% from chitosan-coated MSNs after 48 h, followed by only a slight increase up to 100 h. In both studies, a considerable proportion of the encapsulated curcumin remained retained within the carrier throughout the release period, confirming the ability of silica-based nanocarriers to provide sustained release of hydrophobic compounds. However, unlike the chitosan-coated MSNs developed by Ahmadi Nasab et al., the present formulation incorporates curcumin-loaded MSNs into an injectable thermoresponsive CS/βGP hydrogel, providing an additional diffusion barrier after in situ gelation. This dual carrier system is expected to enhance local drug retention while minimizing the initial burst release, making it more suitable for localized sustained drug delivery applications.

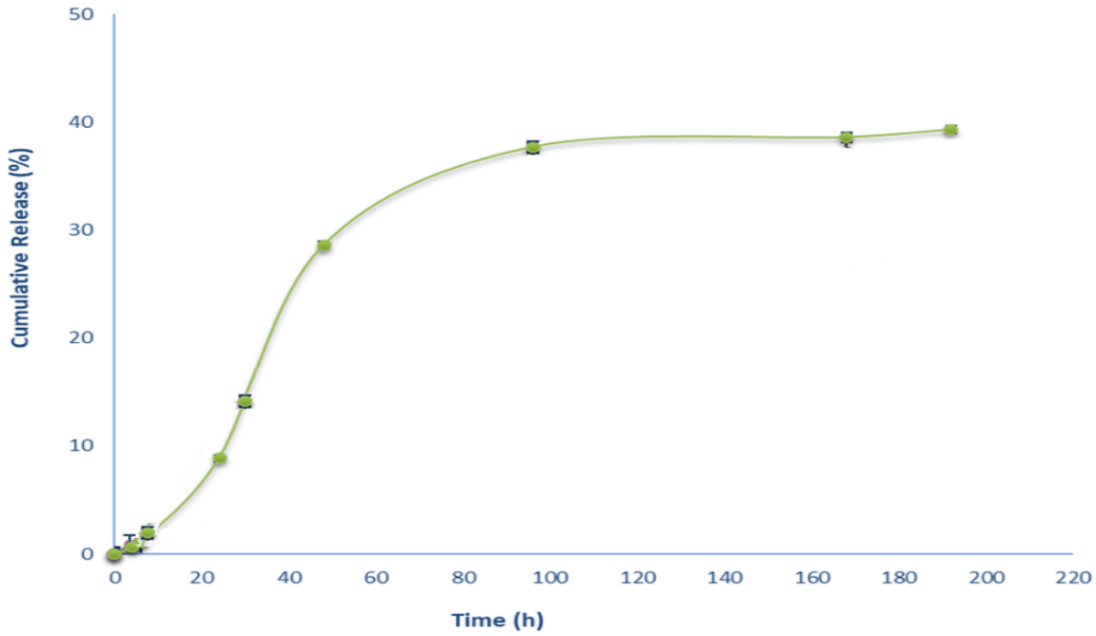

Fig. 6. Cumulative release study of curcumin from CS/βGP/MSNs-CU.

The prolonged release behavior of the CS/βGP/MSNs-CU system can be attributed to several complementary mechanisms. First, curcumin can interact with the amino and hydroxyl groups of the chitosan network through hydrogen bonding, thereby reducing its diffusion rate from the hydrogel matrix. Second, encapsulation of curcumin within the mesoporous channels of silica nanoparticles introduces an additional diffusion barrier, resulting in slower drug transport than free curcumin. Furthermore, the thermally induced CS/βGP hydrogel forms a three-dimensional polymeric network that restricts penetration of the release medium and further retards drug diffusion. Collectively, these structural characteristics account for the sustained release behavior observed under physiological conditions.

To further elucidate the release mechanism, the cumulative release data were fitted to the Higuchi and Korsmeyer–Peppas kinetic models. The Higuchi model is described by the equation $Q=k_H t^{1/2}$, where Q is the cumulative percentage of drug released at time t and k_H is the Higuchi constant. The Korsmeyer–Peppas model is expressed as $M_t/M_\infty=kt^n$, where K is its constant and n is the release exponent indicative of the release

mechanism. The fitting results are summarized in Table 2. The Higuchi model yielded a rate constant of k_H=3.53 with R^2=0.846. For the Korsmeyer–Peppas model, the release exponent was found to be n=0.57 (R^2=0.856). The value of n lying between 0.45 and 0.89 indicates anomalous (non-Fickian) transport, suggesting that curcumin release is governed by the combined effects of drug diffusion through the mesoporous silica channels and the polymeric network of the thermoresponsive chitosan hydrogel, as well as limited polymer chain relaxation. These findings are consistent with the observed prolonged and sustained release profile with minimal burst effect.

3.5. In Vitro biocompatibility study

The in vitro biocompatibility of MSNs, CS/βGP hydrogel, and CS/βGP/MSNs toward healthy primary HPHMF cells was evaluated using the MTT assay, and the results are presented in Fig. 7a–c. The viability of HPHMF cells was not significantly affected by increasing the concentration of the tested samples or by extending the incubation period from 24 to 48 h.

As shown in Fig. 7, cell viability remained above 90% for all tested formulations, even at the highest concentration after 48 h of incubation, indicating excellent biocompatibility toward healthy fibroblast cells. These findings suggest that neither the MSNs nor the injectable CS/βGP hydrogel induced detectable cytotoxic effects under the experimental conditions.

Table 2. Kinetic parameters of curcumin release from CS/βGP/MSNs-CU hydrogel

Kinetic Model	Equation	Parameters	R^2
Higuchi	$Q=k_H t^{1/2}$	k_H=3.53	0.846
Korsmeyer–Peppas	$M_t/M_\infty=kt^n$	k=0.0258, n=0.57	0.856

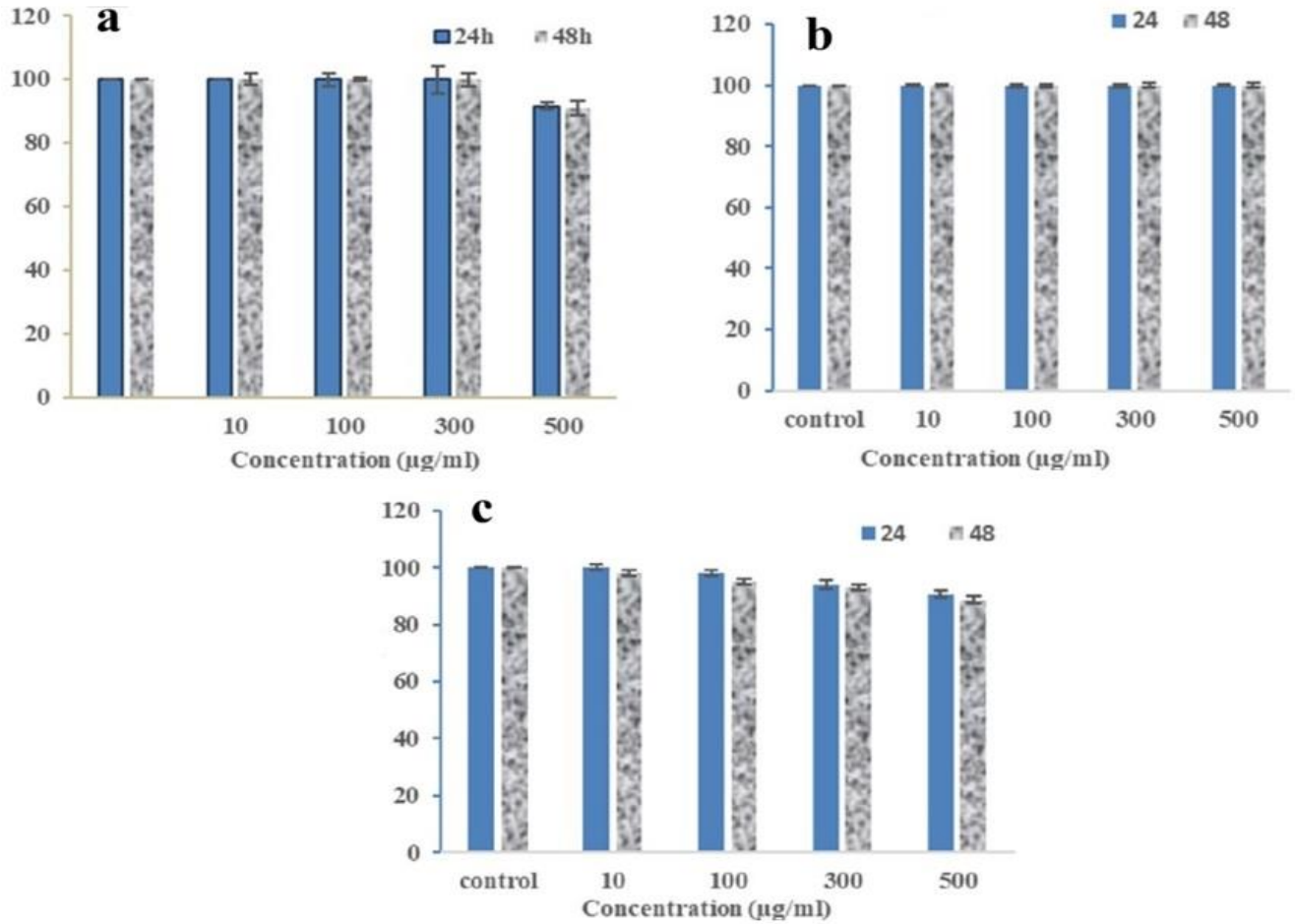

Fig. 7. Biocompatibility of a) MSNs, b) CS/βGP hydrogel and c) CS/βGP/MSNs on HPHMF cells by MTT assay.

The high cell viability can be attributed to the inherent biocompatibility of chitosan and MSNs. The absence of significant cytotoxicity indicates that the developed injectable hydrogel is a promising carrier for sustained drug delivery applications. Furthermore, according to the ISO 10993-5 guideline, materials exhibiting cell viability greater than 70% are generally considered non-cytotoxic. Therefore, the obtained results confirm the favorable biocompatibility of the developed formulations. Although the present study demonstrates excellent biocompatibility toward healthy fibroblasts, further studies using cancer cell lines are required to evaluate the therapeutic efficacy of the developed delivery system. These results are consistent with those reported by Ribeiro et al. [10], who demonstrated the biocompatibility of curcumin-loaded MSNs dispersed in a thermoresponsive hydrogel for intranasal administration. Both studies indicate that incorporation of curcumin-loaded MSNs into thermoresponsive hydrogel systems does not compromise the biological safety of the carrier.

3.6. Cellular uptake analysis

Representative TEM images of MCF-7 cells treated with CS/βGP/MSNs-CU are shown in Fig. 8. Electron-dense nanoparticles were observed within the cellular compartments, confirming the successful internalization of MSNs-CU by MCF-7 cells. The presence of nanoparticles inside the cells indicates that the hydrogel-dispersed MSNs-CU remained available for cellular uptake after incubation. No obvious aggregation of nanoparticles was observed in the examined sections. These findings demonstrate that the developed CS/βGP/MSNs-CU formulation is capable of delivering MSNs to MCF-7 cells under the experimental conditions.

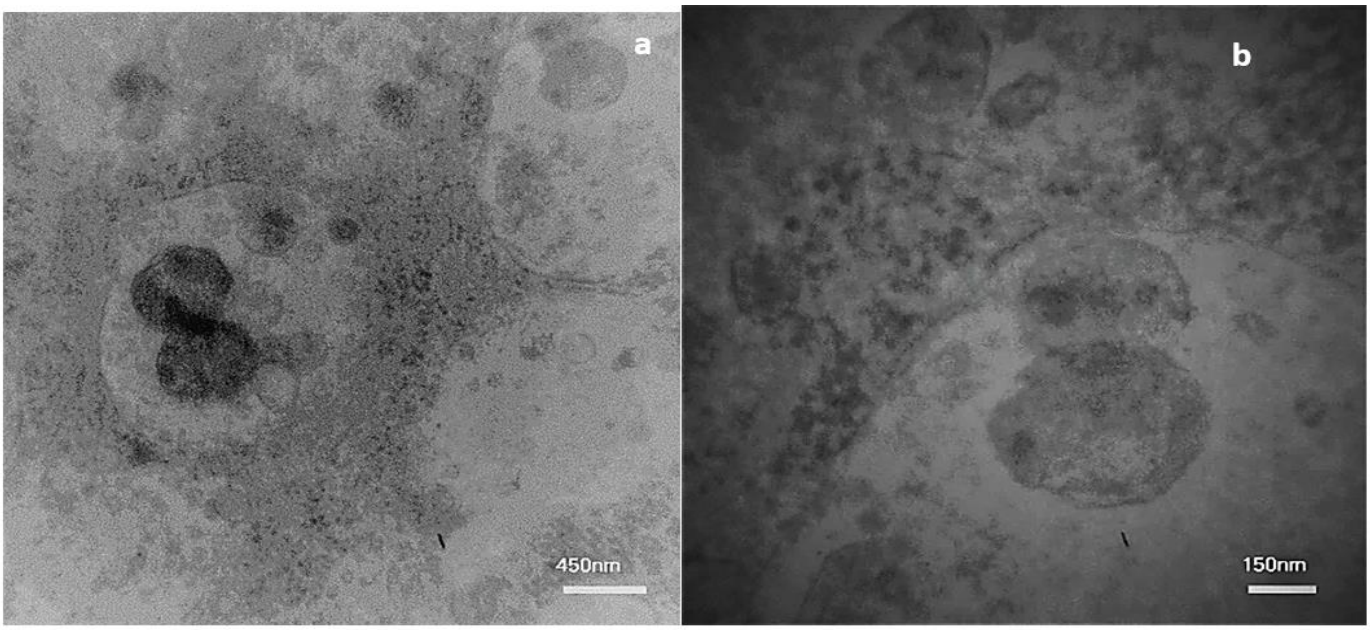

Fig. 8. TEM images of MCF-7 cells after 24 h incubation with CS/βGP/MSNs-CU a) scale bar = 450 nm and (b) scale bar = 150 nm.

It should be noted that TEM analysis provides qualitative evidence of nanoparticle internalization and intracellular localization. However, this technique does not directly quantify the amount of internalized nanoparticles or demonstrate intracellular release of curcumin. Therefore, the present results support successful cellular uptake of the nanoparticle formulation rather than therapeutic efficacy.

Although the present study demonstrated excellent biocompatibility of the developed formulation toward healthy primary human mammary fibroblasts and confirmed the cellular uptake of MSNs-CU by MCF-7 cells, its anticancer efficacy was not investigated. Future studies should evaluate the cytotoxicity and therapeutic performance of the injectable CS/βGP/MSNs-CU hydrogel in relevant cancer cell

13

lines and in vivo tumor models to further explore its potential for localized cancer therapy.

4. CONCLUSIONS

In this study, MSNs-CU were successfully incorporated into an injectable thermoresponsive CS/βGP hydrogel to develop a sustained drug delivery system. Physicochemical characterization confirmed the successful loading of curcumin into the MSNs and their homogeneous incorporation within the hydrogel network. The developed formulation exhibited a prolonged release profile with minimal initial burst release under physiological conditions, demonstrating its potential for sustained local drug delivery.

In vitro biocompatibility studies showed that both MSNs-CU and CS/βGP/MSNs-CU maintained high viability of HPHMF after 24 and 48 h of incubation, indicating favorable biocompatibility. Furthermore, TEM analysis confirmed the successful cellular internalization of the nanoparticles by MCF-7 cells. The observed intracellular localization of MSNs-CU suggests that the developed hydrogel-based formulation can maintain nanoparticle availability for cellular internalization while providing sustained drug release under physiological conditions. Overall, the developed injectable CS/βGP/MSNs-CU hydrogel combines sustained drug release, good biocompatibility, and efficient cellular uptake, suggesting its potential as a localized delivery platform for curcumin and other hydrophobic therapeutic agents. Further in vitro and in vivo studies are warranted to evaluate its therapeutic efficacy and long-term performance.

5. STATEMENTS & DECLARATIONS

5.1. Acknowledgment

The authors would like to acknowledge the assistance of ChatGPT (developed by OpenAI) in refining the English language and grammar of this manuscript. The content and scientific interpretations presented in the article remain entirely the authors' responsibility.

5.2. Funding

The authors declare that no financial support was received for the research, authorship, and/or publication of this article.

5.3. Conflict of Interest

There are no competing interests between the authors.

5.4. Ethics

Consent to Participate declaration

This study doesn't have any human or animal samples.

Clinical Trial Number

Not applicable

Human Ethics &Consent to Participate declarations

This study did not involve human participants or animal experiments. The experiments were performed exclusively using established human cell lines (MCF-7) and commercially available primary human mammary fibroblasts (HPHMF). Therefore, ethical approval and informed consent were not required.

5.5. Author contributions

All authors contributed to the study conception and design. Material preparation, data collection and analysis were performed by Mitra Asadian, Ladan Rashidi and Fariba Ganji. The first draft of the manuscript was written by Mitra Asadian and all authors commented on previous versions of the manuscript. All authors read and approved the final manuscript."

5.6. Data Deposition Information

The datasets generated during and/or analyzed during the current study are available from the corresponding author on reasonable request.

6. REFERENCES

1. Pateiro M, Gómez B, Munekata PES, Barba FJ, Putnik P, Kovačević DB, Lorenzo JM. (2021) Nanoencapsulation of Promising Bioactive Compounds to Improve Their Absorption, Stability, Functionality and the Appearance of the Final Food Products. Molecules. 26(6): 1547. https://doi.org/10.3390/molecules26061547

2. Fuloria S, Mehta J, Chandel A, Sekar M, Rani NNIM, Begum MY, Subramaniyan V, Chidambaram K, Thangavelu L, Nordin R, Wu YS, Sathasivam KV, Lum PT, Meenakshi DU, Kumarasamy V, Azad AK and

Fuloria NK (2022) A comprehensive review on the therapeutic potential of curcuma longa linn. in relation to its major active constituent curcumin. front. Pharmacol. 13: 820806. https://doi.org/10.3389/fphar.2022.820806

3. Omidian H, Wilson RL, Chowdhury SD. (2023) Enhancing Therapeutic Efficacy of Curcumin: Advances in Delivery Systems and Clinical Applications. Gels. 25;9(8):596. https://doi.org/10.3390/gels9080596.

4. Bolouki A, Rashidi L, Vasheghani-Farahani E, Piravi-Vanak Z (2015) Study of Mesoporous Silica Nanoparticles as Nanocarriers for Sustained Release of Curcumin**.** Int J Nanosci Nanotech. 11: 139-146.

5. Almatroudi A. (2025) Advances in Mesoporous Silica and Hybrid Nanoparticles for Drug Delivery: Synthesis, Functionalization, and Biomedical Applications. *Pharmaceutics*. 17(12):1602. https://doi.org/10.3390/pharmaceutics17121602

6. Ahmadi F, Sodagar-Taleghani A, Ebrahim-nejad P, Pouya Hadipour Moghaddam S, Ebrahim-nejad F, Asare-Addo K, Nokhodchi A. (2022) A review on the latest developments of mesoporous silica nanoparticles as a promising platform for diagnosis and treatment of cancer. Int J Pharm. 25;625:122099. https://doi.org/10.1016/j.ijpharm.2022.122099.

7. Rashidi L, Vasheghani Farahani E, Ganji F, Rahmani A, Mazaheri M (2025) Amine-functionalized-mesoporous silica nanoparticles by various pore sizes containing gallic acid: characterization and cytotox-icity effect, Iran. J. Chem. Chem. Eng. 44(02): 336-349.https://doi.org/10.30492/ijcce.2025.2036880.6720

8. Iraji S, Ganji F, Rashidi L (2018) Surface modified mesoporous silica nanoparticles as sustained-release gallic acid nano-carriers. J Drug Del Sci Technol. 47: 468–476.

9. Rashidi L, Vasheghani-Farahani E, Soleimani M, Atashi A, Rostami K, Gangi F, Fallahpour M, Tahouri MT (2014) A cellular uptake and cytotoxicity properties study of gallic acid-loaded mesoporous silica nanoparticles on Caco-2 cells. J Nanopart Res. 16: 132-145. https://doi.org/10.1007/s11051-014-2285-6.

10. Ribeiro TdC, Sábio RM, Luiz MT, de Souza LC, Fonseca-Santos B, Cides da Silva LC, Fantini MCdA, Planeta CdS, Chorilli M. (2022) Curcumin-Loaded Mesoporous Silica Nanoparticles Dispersed in Thermo-Responsive Hydrogel as Potential Alzheimer Disease Therapy. *Pharmaceutics*. 14(9): 1976. https://doi.org/10.3390/pharmaceutics14091976.

11. Gonciarz W, Balcerczak E, Brzeziński M, Jeleń A, Pietrzyk-Brzezińska AJ, Narayanan VHB, Chmiela M. Chitosan-based formulations for therapeutic applications. A recent overview. J Biomed Sci. 2025 Jul 8;32(1):62. https://doi.org/10.1186/s12929-025-01161-7.

12. Ahmadi Nasab N, Hassani Kumleh H, Beygzadeh M, Teimourian S, Kazemzad M (2018) Delivery of curcumin by a pH-responsive chitosan mesoporous silica nanoparticles for cancer treatment. Artif**.** Cells Nanomed Biotechnol**.** 46: 75-81. https://doi.org/10.1080/21691401.2017.1290648.

13. Wang J, Huang L, Wu E, Li X, Rao Y, Zhu C. Recent Advances on Chitosan-Based Thermosensitive Hydrogels for Skin Wound Treatment. *Biology*. 2025; 14(6):619. https://doi.org/10.3390/biology14060619

14. Kazemi-Aghdam F., Jahed V., Dehghan-Niri M., Ganji F., Vasheghani-Farahani E., (2021), Injectable chitosan hydrogel embedding modified halloysite nanotubes for bone tissue engineering, Carbohydrate Polymer, 269, 118311. https://doi.org/10.1016/j.carbpol.2021.118311

14. Ghapanvari MA, Ganji F, Shaki H, Jafarzadeh-Holagh S, Vashegani-Farahani E, (2025) Bone-targeted and redox-responsive polymeric nanomicelles based on hyaluronic acid, Int J Pharmaceut, 679, 125734. https://doi.org/10.1016/j.ijpharm.2025.125734

15. Jangle RD, Thorat BN (2017) Reversed-phase High-performance Liquid Chromatography Method

for Analysis of Curcuminoids and Curcuminoid-loaded Liposome Formulation. Indian J Pharm Sci. 1: 60-67.

16. Hu X, Wang Y, Peng B (2014) Chitosan-Capped Mesoporous Silica Nanoparticles as pH-Responsive Nanocarriers for Controlled Drug Release. Chem Asian J. 9: 319-327. https://doi.org/10.1002/asia.201301105.

17. Yaghoubzadeh, Z, Safari, R., Soheili, M. (2025) Cytotoxicity activity of peptides derived from enzymatic hydrolysis of Chlorella vulgaris proteins. *Applied Food Biotechnology*, *12*(1), 1–9 (e1). https://doi.org/10.22037/afb.v12i1.46685

18. Tiwari N, Nawale L, Sarkar D, Badiger MV (2017) Carboxymethyl Cellulose-Grafted Mesoporous Silica Hybrid Nanogels for Enhanced Cellular Uptake and Release of Curcumin. Gels. 3: 1-15. https://doi.org/10.3390/gels3010008.

19. Daryasari MP, Akhgar MR, Mamashli F, Bigdeli B, Khoobi M (2016) Chitosan-folate coated mesoporous silica nanoparticles as a smart and pH-sensitive system for curcumin delivery. RSC Adv. 6: 105578-105588.